

# Correlation of *in vivo* photosensitizer fluorescence and photodynamic-therapy-induced depth of necrosis in a murine tumor model

## Rex Cheung\*

University of Pennsylvania  
Department of Physics and Astronomy  
and Department of Radiation Oncology  
Philadelphia, Pennsylvania 19104

## Michael Solonenko

University of Pennsylvania  
Department of Physics and Astronomy  
and Department of Radiation Oncology  
Philadelphia, Pennsylvania 19104

## Theresa M. Busch

University of Pennsylvania  
Department of Radiation Oncology  
Philadelphia, Pennsylvania 19104

## Fabio Del Piero

University of Pennsylvania  
Department of Pathobiology  
Philadelphia, Pennsylvania 19104

## M. E. Putt

University of Pennsylvania  
Department of Biostatistics and Epidemiology  
Philadelphia, Pennsylvania 19104

## Stephen M. Hahn

University of Pennsylvania  
Department of Radiation Oncology  
Philadelphia, Pennsylvania 19104

## Arjun G. Yodh

University of Pennsylvania  
Department of Physics and Astronomy  
and Department of Radiation Oncology  
Philadelphia, Pennsylvania 19104  
E-mail: yodh@dept.physics.upenn.edu

**Abstract.** We compared light-induced fluorescence (LIF) to nominal injected drug dose for predicting the depth of necrosis response to photodynamic therapy (PDT) in a murine tumor model. Mice were implanted with radiation-induced fibrosarcoma (RIF) and were injected with 0, 5, or 10 mg/kg Photofrin. 630-nm light ( $30 \text{ J/cm}^2$ ,  $75 \text{ mW/cm}^2$ ) was delivered to the tumor after 24 hours. Fluorescence emission ( $\lambda_{\text{excitation}} = 545 \text{ nm}$ ,  $\lambda_{\text{emission}} = 628 \text{ nm}$ ) from the tumor was measured. The LIF data had less scatter than injected drug dose, and was found to be at least as good as an injected drug dose for predicting the depth of necrosis after PDT. Our observations provide further evidence that fluorescence spectroscopy can be used to quantify tissue photosensitizer uptake and to predict PDT tissue damage. © 2003 Society of Photo-Optical Instrumentation Engineers. [DOI: 10.1117/1.1560011]

Keywords: spectroscopy; photodynamic therapy; light-induced fluorescence; necrosis; photofrin; radiation-induced fibrosarcoma tumor; dosimetry.

Paper 02019 received Mar. 12, 2002; revised manuscript received Aug. 27, 2002; accepted for publication Nov. 14, 2002.

## 1 Background

Photodynamic therapy (PDT) is a cancer therapy that uses nonionizing photons and a photosensitizer to treat solid tumors and surface malignancies.<sup>1</sup> The efficacy of PDT depends on the simultaneous presence of photosensitizer, light, and oxygen. Visible light is used to excite the photosensitizer. This excitation initiates a cascade of chemical reactions, involving highly reactive oxygen intermediates that produce cellular damage.<sup>1</sup>

Models for the photodynamic dosimetry offer a quantitative basis for the improvement of PDT treatment protocols, and require accurate measurements of tissue optical properties for their implementation. In the explicit dosimetry method,<sup>2</sup> the PDT threshold dose is defined as the minimum number of photons absorbed by the photosensitizer per unit tissue volume required to produce tissue necrosis. By contrast, an im-

PLICIT PDT dosimetry model<sup>3</sup> relies on the measurement of a variable that depends sensitively on a range of the response-determining treatment factors. In theory such measurements eliminate the need to measure all other tissue factors explicitly. Variation in the fluorescence emission of a photosensitizer, for example, can in some instances be correlated with tissue response and is thus a leading candidate for implicit dosimetry.

At the University of Pennsylvania, we are carrying out clinical trials with PDT for treatment of peritoneal sarcoma,<sup>4</sup> malignant pleural effusion, mesothelioma, and recurrent prostate cancer. It is well known that there are substantial variations in drug uptake and light dose distribution in biological systems.<sup>5</sup> Several groups have investigated tissue fluorescence as a surrogate for actual tissue drug concentration, as a predictor of PDT tissue response.<sup>6–9</sup> In the present study we used before-PDT fluorescence as a means to characterize tis-

\*Current affiliation: U.T. MD Anderson Cancer Center, 1515 Holcombe Boulevard, Box 97, Houston, TX 77030-4009.

sue drug concentration. We then correlated the laser-induced fluorescence (LIF) and the nominal injected drug dose with PDT-induced depth of necrosis, and with each other.

## 2 Study Design, Materials, and Methods

### 2.1 Mouse Tumor Model

The radiation-induced fibrosarcoma (RIF) tumor cell line was maintained according to strict protocol of *in vitro* and *in vivo* passages as described earlier.<sup>10</sup> For *in vivo* studies, the RIF tumor was implanted on the shoulders of female C3H mice (average weight 21.2 g) (Taconic, Germantown, New York) by intradermal injection of  $3 \times 10^5$  cells. Tumors were treated about one week after injection, at a size of about 5 to 7 mm in diameter. At that size, all tumors were free of visible necrosis.

### 2.2 Assessment of PDT Tissue Damage

Mice were injected with 0 ( $n=2$ ), 5 ( $n=3$ ), and 10 ( $n=3$ ) mg/kg Photofrin (QLT Phototherapeutics Incorporated Vancouver, B.C., Canada) IV via tail veins. Light was delivered to the tumor 24 hours after drug injection using the emission of a KTP-YAG-pumped Rhodamine 6G dye laser (Laser-scope model XP, San Jose, California) operating at 630 nm with a Microlens output optical fiber (Rare Earth Medical, West Yarmouth, Massachusetts). The fluence rate was 75 mW/cm<sup>2</sup>, and the total delivered light dose was 30 J/cm<sup>2</sup>. Incident light intensity was measured by standard power meters (Coherent, Auburn, California). Prior to PDT, mice were anesthetized by an intraperitoneal injection of ketamine/xylazine (175/10 mg/kg).

To assess the tissue damage by PDT in the RIF murine tumor, we adopted a procedure similar to the work of Fingar et al.<sup>11</sup> At 24 hours after PDT treatment, tumors were excised and fixed. They were cut in half vertically with respect to the skin surface, and stained with hematoxylin-eosin. Measurements of the depth of necrosis from the skin inward were made on a graded reticule (microns) using light microscopy by our pathologist who was blinded to the injection dose and to the fluorescence signal. For each excised tumor, three to five sections were taken near the midline. There were no significant variations in the depths of necrosis. We are using the deepest depth of necrosis in each tumor in this work.

### 2.3 Fluorescence/Absorption Spectroscopy

We have developed an apparatus that may be used for both fluorescence and absorption measurements (Fig. 1). Incident light for absorption measurements was derived from a lamp source. The instrument was converted into a fluorescence spectrometer by using an interference bandpass filter (Oriel) to select our desired excitation light [545 nm,  $\sim 20$  nm full-width half maximum (FWHM)] from the total lamp output. Detection was accomplished using a fiber-optic probe made of 32 fibers placed in a line with 0.24-mm separation between their centers. The distance between the source and the first detection fiber was 0.44 mm.

Data analysis algorithms were developed using LabView® graphical programming language (National Instruments, Austin, Texas). We estimated the effective attenuation coefficient  $\mu_{\text{eff}}$  of the tumor tissue based on the absorption signals collected by detectors located 1.16 to 5 mm from the source. To

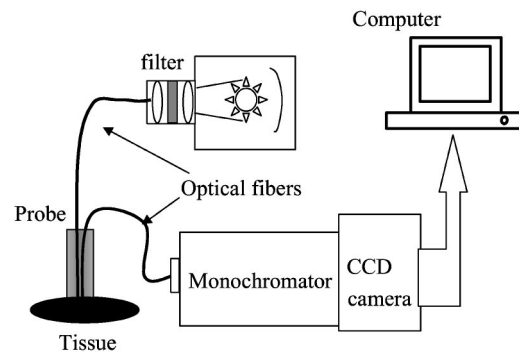


**Fig. 1** Schematic of the experimental setup for the light-induced fluorescence measurements. The instrument consists of three parts: the CCD camera, wavelength dispersion system (monochromator), and fiber optics probe head.

solve for  $\mu_{\text{eff}}$ , we assumed the diffusion approximation for light transport was valid, and fit our reflectance data using the semi-infinite medium approximation<sup>12</sup>

$$I(\rho) = (A/\rho^2) \exp(-\rho\mu_{\text{eff}}). \quad (1)$$

Here,  $I(\rho)$  is the reflected light intensity at distance  $\rho$  from the source, and  $A$  is proportional to the incident light intensity at the entrance into the tumor tissue. Plots of  $\ln[\rho^2 I(\rho)]$  versus  $\rho$  yield  $\mu_{\text{eff}}$  as the slope. The optical penetration depth  $\delta = 1/\mu_{\text{eff}}$ .

Our probe arrangement allowed us to enhance the LIF signals by integrating over several consecutive detectors. In our case, LIF signals from the first three fibers were used. The fluorescence measurements were typically obtained in less than a second. Approximately 200 nW of light from a tungsten halogen lamp was coupled into the tissue using one 210- $\mu\text{m}$  core diameter multimode source fiber. The detection fibers collected the LIF and transported the light emission to the entrance slit of the imaging monochromator (300 gr/mm,  $f\# = 4$ , Acton Research, Acton, Massachusetts). The spectra were collected before and after light delivery concurrently in the range of 500 to 900 nm using a liquid nitrogen cooled CCD camera (Princeton Instruments, 16 bit, 24- $\mu\text{m}$  pixel size, 330  $\times$  1100 pixels) that operated at 163 K.

The LIF signal was smoothed and normalized at 615 nm. The normalization corrected for variation of the incident light power. The fluorescence spectra contained a combination of autofluorescence and Photofrin fluorescence. To monitor tissue uptake, the Photofrin fluorescence (peak 628) was integrated between 615 and 645 nm (Fig. 2). In this range, the Photofrin fluorescence was clearly distinguishable from tissue autofluorescence in the control mice [Fig. 3(a)].

Statistical analysis was performed using routines provided by SPSS (SPSS Incorporated, Chicago, Illinois) and Excel (Microsoft Corporation).

## 3 Results and Discussion

### 3.1 Tissue Photofrin Concentration with LIF Spectroscopy

Fluorescence spectroscopy is rapidly approaching clinical use in many contexts.<sup>13,14</sup> For example, fluorescence microscopy

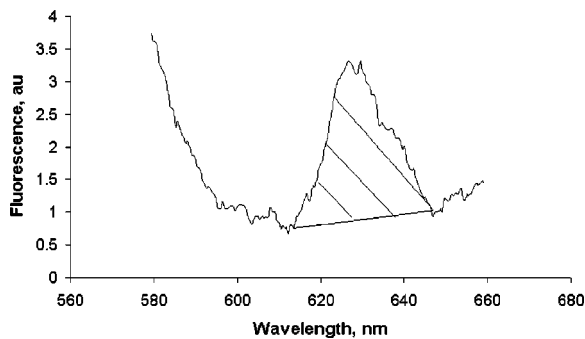


**Fig. 2** Calculation of LIF signal of tissue Photofrin. The overall signal consists of autofluorescence and the LIF. Excitation wavelength was 545 nm. The Photofrin fluorescence was integrated from 615 to 645 nm (hatched area).

makes possible a detailed examination of drug deposition in cells and tumor tissue.<sup>15</sup> We have explored the utility of macroscopic LIF spectroscopy for providing semi-quantitative measures of tissue Photofrin uptake, and we correlated fluorescence measurements with the PDT-induced tissue depth of necrosis.

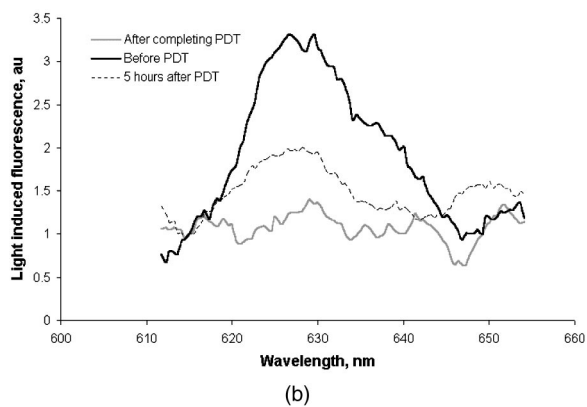
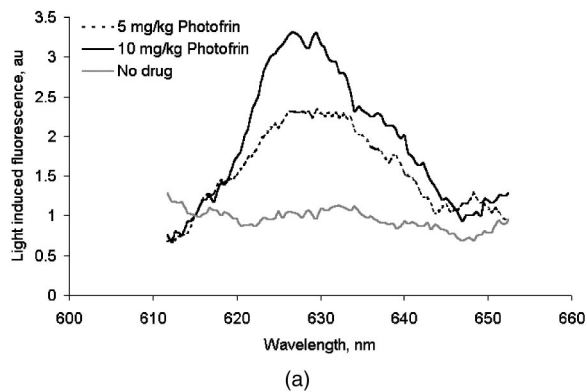


**Fig. 3** (a) *In-vivo* LIF monitoring of tissue Photofrin uptake showing LIF signal increases with the amount of Photofrin injected. The mice were injected with 0, 5, and 10 mg/kg Photofrin, respectively, 24 hours prior to these measurements. (b) Photobleaching of Photofrin immediately after PDT, and partial replenishment of Photofrin LIF after five hours. The spectra were obtained from a mouse injected with 10 mg/kg Photofrin.

Absolute quantification of drug fluorescence is complex and requires attention to photon transport physics and photobiology. Tissue optical properties affect the true light dose at specific locations below the tissue surface, and can complicate the interpretation of tissue fluorescence measurements. The latter effect arises because the source distribution of excitation light depends on tissue optical properties at the excitation wavelength, and because propagation of the fluorescent photons depends on tissue optical properties at the emission wavelength. Despite these difficulties, absolute determination of drug concentration in a semi-infinite phantom based on LIF has been reported.<sup>16,17</sup>

*In-vivo* use of these methods is complicated and is under active investigation.<sup>2,18</sup> For example, in PDT of early stage carcinomas of the esophagus with tetra(meta-hydroxyphenyl)chlorin (mTHPC), investigators have found large variations of mTHPC uptake among patients.<sup>8</sup> Fluctuations in the degree of tumor destruction between patients were found to be related to mucosal drug uptake as measured by LIF,<sup>8</sup> suggesting that LIF may be used as a guide for PDT. By using LIF as a measure of tissue photosensitizer concentration, these investigators improved the predictability of PDT-induced tumor destruction. This earlier study suggested that the PDT-induced tissue damage was also dependent on the fluence rate. In the research, we quantify tissue damage by measuring the depth of necrosis at a fixed fluence rate that is commonly used in PDT.

### 3.2 Depth of Light Penetration

Figure 3(a) shows the *in vivo* Photofrin LIF spectra from tumors on three mice with 0, 5, and 10 mg/kg tail vein IV injection of drug, respectively. In our murine tumor model, the Photofrin fluorescence peaks at 628 nm were clearly measurable (Fig. 2). From our absorption measurements, we calculated the optical depth of penetration  $\delta$  at 630 nm.  $\delta$  was  $6.3 \pm 1.2$  mm. The data on PDT-induced necrosis suggest that different depths of therapeutic light penetration did not significantly correlate with the depth of necrosis. The Pearson correlation coefficients between  $\delta$  and depth of necrosis was 0.295.

### 3.3 Quantification of Tissue Photofrin Uptake

Assuming the drug distribution was uniform, we estimated<sup>19</sup> the source of our fluorescence signal was predominantly from depths of order  $0.4 \pm 0.2$  mm. Our measured Photofrin fluorescence peak is consistent with what other investigators have observed.<sup>20</sup> In the control mice (without Photofrin injection), LIF signals and tissue necrosis were negligible (Fig. 4). This is consistent with known observations that conditions with either light or drug alone are not enough to cause tissue necrosis; a combination of the two is required.<sup>21</sup> The Pearson correlation between the injected drug dose and the LIF signals was high with a coefficient of 0.875. Based on the LIF measurements, we observed that tissue Photofrin uptake may vary with the same injected doses at 5 or 10 mg/kg. In our case it was especially true for mice injected with 5 mg/kg Photofrin (Fig. 4). The mice received Photofrin via tail vein injection; success of the injection was readily monitored visually. Therefore, we postulate that variation in tissue Photofrin concentration was largely due to tumor uptake. The sources of variable tumor uptake, which may include factors such as tumor angiogenesis and metabolic level, will require further

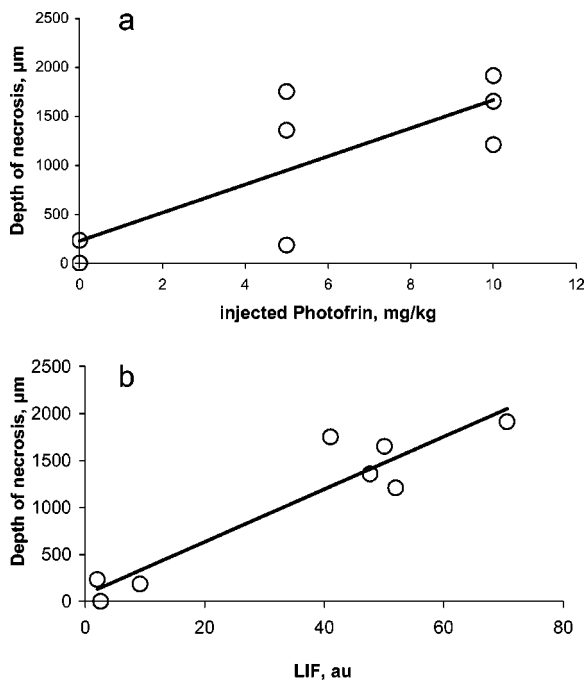


**Fig. 4** Fit of depth of necrosis to injected Photofrin dose in (a) mg/kg and (b) to LIF.

investigation. However, Figs. 3(a) and 3(b) suggest the background fluorescence in both the tumor and the normal tissue is minimal and is unlikely to be the source of the observed variation. Our data suggest that the pre-PDT LIF intensity is an indicator of average drug concentration in the tumor and is critical for PDT-induced tissue necrosis.

Photobleaching is a well-known phenomenon in PDT. LIF spectroscopy is capable of rapid *in-situ* monitoring of tissue photosensitizer concentration. The temporal dynamics of photosensitizer bleaching during PDT has been studied<sup>7</sup> and has provided insight about fractionation of the PDT light dose. Such experiments force us to reevaluate treatment protocols on a fundamental level.<sup>22,23</sup> In this study, we also observed significant photobleaching after the PDT in the murine tumor model [Fig. 3(b)]. The maximum photobleaching was about 85%, and interestingly, about 30% of the LIF signals replenished 4 hours after PDT (data not shown). The background fluorescence as seen after PDT was small [Fig. 3(a)], indicating that the fluorescence peak represented the tissue Photofrin uptake.

### 3.4 Comparison of LIF and Drug Dose for Prediction of Depth of Necrosis

The Pearson correlation coefficient between the nominal drug dose and depth of necrosis was 0.771. The correlation coefficient increased to 0.941 using LIF signals as a measure of tissue Photofrin concentration. Figure 4 shows the results of linear regression using LIF and injected drug dose with respect to predicting depth of necrosis. The goodness of fit measure R-square is superior for LIF (0.86) compared to the injected drug dose (0.59). While suggestive, we note that our

sample size is rather small; further work must be done to conclude that LIF is more predictive of the depth of necrosis than the injected drug dose.

Finally, we observed variability in depth of tissue necrosis by PDT at the same nominal drug dose (Fig. 4). In particular, mouse 4 has much less tissue necrosis than the other mice injected with 5 mg/kg Photofrin (Fig. 4). Using LIF spectroscopy, mouse 4 was found to have low tissue Photofrin uptake, possibly accounting for the low degree of necrosis. To rule out the possibility of mouse 4 skewing the statistics, we also calculated the correlation coefficients omitting mouse 4. The Pearson correlation coefficients between the nominal drug dose to the depth of necrosis was 0.831. The correlation coefficient improved to 0.930 using LIF signals as a measure of tissue Photofrin concentration.

## 4 Conclusion

Even with our relatively small sample size, we have found that LIF spectroscopy can be used to monitor tissue Photofrin uptake, and can be used to predict tissue depth of necrosis. The results suggest that real time *in-situ* LIF measurements may facilitate the individualized choice of an optimal PDT drug and light dose.

### Acknowledgments

We thank Dr. W. Gillies McKenna and Dr. Eli Glatstein for support and encouragement, and Dr. Cecil Cheung and Dr. Joe Culver for helpful discussions. We thank Ms. Aimee Torres for technical support. A.G.Y. acknowledges support of the NIH through a grant #HL57835-01, and NIH grant #P01 CA87971.

### References

1. T. J. Dougherty, C. J. Gomer, B. W. Henderson, G. Jori, D. Kessel, M. Korbelik, J. Moan, and Q. Peng, "Photodynamic therapy," *J. Natl. Cancer Inst.* **90**, 889–905 (1998).
2. T. J. Farrell, B. C. Wilson, M. S. Patterson, and M. C. Olivo, "Comparison of the *in vivo* photodynamic threshold dose for photofrin, mono- and tetrasulfonated aluminum phthalocyanine using a rat liver model," *Photochem. Photobiol.* **68**, 394–399 (1998).
3. B. C. Wilson, M. S. Patterson, and L. Lilge, "Implicit and explicit dosimetry in photodynamic therapy: a new paradigm," *Lasers Med. Sci.* **12**, 182–192 (1997).
4. T. W. Bauer, S. M. Hahn, F. R. Spitz, A. Kachur, E. Glatstein, and D. L. Fraker, "Preliminary report of photodynamic therapy for intraperitoneal sarcomatosis," *Ann. Surg. Oncol.* **8**, 254–259 (2001).
5. *Photodynamic Therapy of Neoplastic Disease*, Vols. I, II, D. Kessel, Ed., CRC Press, Boca Raton, FL (1990).
6. H. Barr, C. J. Tralau, P. B. Boulos, A. J. MacRobert, N. Krasner, D. Phillips, and S. G. Bown, "Selective necrosis in dimethylhydrazine-induced rat colon tumors," *Gastroenterology* **98**, 1532–1537 (1990).
7. D. J. Robinson, H. S. de Bruijn, N. van der Veen, M. R. Stringer, S. B. Brown, and W. M. Star, "Fluorescence photobleaching of ALA-induced protoporphyrin IX during photodynamic therapy of normal hairless mouse skin: the effect of light dose and irradiance and the resulting biological effect," *Photochem. Photobiol.* **67**, 140–149 (1998).
8. D. Braichotte, J. F. Savary, P. Monnier, and H. E. van den Bergh, "Optimizing light dosimetry in photodynamic therapy of early carcinomas of the esophagus using fluorescence spectroscopy," *Lasers Surg. Med.* **19**, 340–346 (1996).
9. J. S. Dysart, M. S. Patterson, T. J. Farrell, and G. Singh, "Relationship between mTHPC fluorescence photobleaching and cell viability during *in vitro* photodynamic treatment of DP16 cells," *Photochem. Photobiol.* **75**, 289–295 (2002).
10. T. M. Busch, S. M. Hahn, S. M. Evans, and C. J. Koch, "Depletion of

- tumor oxygenation during photodynamic therapy: detection by the hypoxia marker EF3 [2-(2-nitroimidazol-1-[H]-yl)-N-(3,3,3-trifluoropropyl)acetamide]," *Cancer Res.* **60**, 2636–2642 (2000).
11. V. H. Fingar, T. J. Wieman, S. A. Wiehle, and P. B. Cerrito, "The role of microvascular damage in photodynamic therapy: the effect of treatment on vessel constriction, permeability, and leukocyte adhesion," *Cancer Res.* **52**, 4914–4921 (1992).
  12. T. J. Farrell, M. S. Patterson, and B. Wilson, "A diffusion theory model of spatially resolved, steady-state diffuse reflectance for the noninvasive determination of tissue optical properties in vivo," *Med. Phys.* **19**, 879–888 (1992).
  13. I. Georgakoudi, B. C. Jacobson, J. Van Dam, V. Backman, M. B. Wallace, M. G. Muller, Q. Zhang, K. Badizadegan, D. Sun, G. A. Thomas, L. T. Perelman, and M. S. Feld, "Fluorescence, reflectance, and light-scattering spectroscopy for evaluating dysplasia in patients with Barrett's esophagus," *Gastroenterology* **120**, 1620–1629 (2001).
  14. M. Brewer, U. Utzinger, E. Silva, D. Gershenson, R. C. J. Bast, M. Follen, and R. Richards-Kortum, "Fluorescence spectroscopy for in vivo characterization of ovarian tissue," *Lasers Surg. Med.* **29**, 128–135 (2001).
  15. K. W. Woodburn, Q. Fan, D. R. Miles, D. Kessel, Y. Luo, and S. W. Young, "Localization and efficacy analysis of the phototherapeutic lutetium texaphyrin (PCI-0123) in the murine EMT6 sarcoma model," *Photochem. Photobiol.* **65**, 410–415 (1997).
  16. B. W. Pogue and G. Burke, "Fiber-optic bundle design for quantitative fluorescence measurement from tissue," *Appl. Opt.* **37**, 7429–7439 (1998).
  17. M. Canpolat and J. R. Mourant, "Monitoring photosensitizer concentration by use of a fiber-optic probe with a small source-detector separation," *Appl. Opt.* **39**, 6508–6514 (2000).
  18. M. S. Patterson, B. C. Wilson, and R. Graff, "In vivo tests of the concept of photodynamic threshold dose in normal rat liver photosensitized by aluminum chlorosulphonated phthalocyanine," *Photochem. Photobiol.* **51**, 343–349 (1990).
  19. X. D. Li, M. A. O'Leary, D. A. Boas, B. Chance, and A. G. Yodh, "Fluorescent diffuse photon density waves in homogeneous and heterogeneous turbid media: analytic solutions and applications," *Appl. Opt.* **35**, 3746–3758 (1996).
  20. J. Moan, K. Berg, and V. Iani, "Action spectra of dyes relevant for photodynamic therapy," in *Photodynamic Tumor Therapy*, J. G. Moser, Ed., pp. 169–182, The Gordon and Breach Publishing Group, Amsterdam, The Netherlands (1998).
  21. W. M. Star, H. P. A. Marijnissen, A. E. van den Berg-Blok, J. A. C. Versteeg, K. A. P. Franken, and H. S. Reinhold, "Destruction of rat mammary tumor and normal tissue microcirculation by hematoporphyrin derivative photoradiation observed in vivo in sandwich observation chambers," *Cancer Res.* **46**, 2532–2540 (1986).
  22. I. Georgakoudi, M. G. Nichols, and T. H. Foster, "The mechanism of Photofrin photobleaching and its consequences for photodynamic dosimetry," *Photochem. Photobiol.* **65**, 135–144 (1997).
  23. N. Van der Veen, H. S. De Bruijn, and W. M. Star, "Photobleaching during and reappearance after photodynamic therapy of topical ALA-induced fluorescence in UVB-treated mouse skin," *Int. J. Cancer* **72**, 110–118 (1997).